

# A Novel Modelling Approach for Wireless Infrared Links

Dimitrios Mavrakis and Simon R. Saunders

Centre for Communication Systems Research  
University of Surrey  
Guildford, Surrey, GU2 7XH, Great Britain  
Email: {D.Mavrakis, S.Saunders}@eim.surrey.ac.uk

*Abstract*— In this paper we present a novel method for calculating the Impulse Response of the wireless diffuse infrared channel. This method involves modelling around the delays that are associated within the specific configuration of the channel and the FOV of both receiving and transmitting elements. The approach involves both Lambertian and specular scatterers. Finally, we present results for specular and line of sight cases, for both Lambertian and specular scatterers, and reach the conclusion that specular scattering yields totally different results and cannot be ignored.

*Keywords*: Infrared, Propagation Modelling, diffuse, specular

## I. INTRODUCTION

Optical communications now allow not only the simple interconnection of two devices, but high bit-rate wireless communication. They offer great advantages over radio. Namely, the infrared spectrum is not governed by a regulating body and so, enormous bandwidths are available. Also, the effective area of the receiving element is many orders greater than the wavelength, eliminating multipath fading [1]. On the other hand, multipath dispersion is present and degrades the system. The need for careful modelling of the channel is large, since a high-rate system will not allow margins for channel modelling errors.

### I.1 Previous Models

Previous infrared propagation modelling approaches involved discretising the rooms into elementary surfaces ('facets') and calculating the differential powers and delays between all of them. This approach, known as radiosity [2], is widely used in image processing and ray tracing and involves the radiant exchange between two surfaces. The centre of each facet is considered, and the smaller they are, the better the resolution of the simulation. This approach may seem to be the most accurate, but it is very expensive in calculation time and processing power. In many cases, facets, which contribute to non-important parts of the impulse response have to be considered, thus leading to very long simulation times. As an example [3], a simulation of a room with 2776 facets, taking into account up to 4 reflections takes about 7.5 years even with a powerful computer.

Many attempts have been made in order to make

this technique faster, and most of them are based on improving the efficiency of the simulation by parallelising the facet calculations [4]. Other approaches that simplify modelling use exponential decay models [5] but are not as accurate and can only be used for a small number of reflections. Ray tracing has also been used [6] but is also computationally intensive since a large number of rays has to be fired for accuracy. More exotic approaches such as neural networks [7] and statistical modelling [8] have been presented, but none have quite reached to goal of making the simulation as fast, efficient and reliable.

In this paper, a new technique is presented, in which the room is not discretised into facets. In section 2, the reflection models are described and in section 3, the simulation model is analysed. Results are presented in section 4, and the conclusions in section 5.

## II. PREVIOUS MODELS

At this point of the analysis, only rectangular rooms have been simulated. These rooms are almost always found in typical office environments, where the need for high-bit rate communication is more necessary than any other area. These models can be expanded to include furniture, but in this paper, only empty rooms are considered.

### II.1 Reflection Models

In order to create a propagation model that takes into account reflections from walls, a suitable reflection model has to be employed. In the past, only the Lambertian model has been used, which has proven to be adequate [9]. In some cases though, where high-reflectivity materials are used, such as mirrors or glass, the Lambertian model does not hold, since the reflection is mainly specular. Hence the Phong model [10] is used, which accounts for both types of reflection.

The Lambertian model is described by the following equation:

$$P_t(\theta) = \frac{n+1}{2\pi} P_r \rho \cos(\theta) \quad (1)$$

where  $P_t$  is the transmitted power from the surface,  $n$  is the mode number of the source and depends on its

directionality,  $P_r$  is the incident power on the surface,  $\rho$  is the reflectivity of the surface, and  $\theta$  is the angle of observation measured from the normal of the surface.

It is interesting that this model is used both for sources, in which the mode number may vary, and for reflection models, in which the mode number is always unity.

The Phong model is described by the following equation [10]:

$$P_t = \frac{\rho P_r}{\pi} \{r_d \cos(\theta_o) + (1 - r_d) \cos^n(\theta_o - \theta_i)\} \quad (2)$$

where  $P_t$ ,  $P_r$ ,  $\rho$ ,  $\theta_o$  are the same as above,  $r_d$  is the percent of the power that is reflected diffusely, and  $\theta_i$  is the incidence angle, measured with respect to the normal of the surface. The Phong model is only used for reflection modelling and includes Lambert's reflection model, as a special case with  $r_d$  set to unity.

## II.2 Propagation model

The channel obeys the Intensity Modulation/Direct Detection principles of Optical Communications. In these channels, only positive signals can be transmitted, in the form of optical power. The phase is also ignored, since the receiving element spans thousands of wavelengths, and eliminates multipath fading. The most important degradation of the channel is multipath dispersion, which spreads a transmitted pulse across time. This effect is simulated, in order to fully characterise the infrared wireless channel.

As mentioned above, the novel propagation model does not involve discretising the walls of the room into facets, but modelling the channel impulse response with respect to the delays present in the configuration. The next sections describe the channel in more detail.

### II.2.1 Line of sight Component

The only calculation that needs to be done for the line of sight (or zero order impulse response) link, is for the power and delay from transmitter to receiver. Using a simple path loss model is adequate [1], only if the following assumption is made: that the square of the distance between the receiver and transmitter is much larger than the detector's area. The following equation describes the approach:

$$h^{(0)}(t) = \frac{n+1}{2\pi} \cos^n(\phi) d\Omega \text{rect}\left(\frac{\theta}{FOV}\right) \delta\left(t - \frac{R}{c}\right) \quad (3)$$

where

$h^{(0)}(t)$  is the LOS component of the impulse response (1/sec),

$n$  is the mode number of the source,

$\phi$  is the angle between the transmitted ray and the normal to the receiver (deg),

$\theta$  is the angle between the incident ray and the normal to the receiver (deg),

$FOV$  is the Field of View solid angle of the receiver (deg),

$R$  is the distance between the transmitter and receiver (m),

$c$  is the speed of light (m/sec),  $A_R$  is the area of the receiving element ( $m^2$ )

and  $d\Omega$  is the solid angle formed by the receiver's area

$$d\Omega = \frac{\cos(\theta) A_R}{R^2} \quad (4)$$

The rectangular function is defined by:

$$\text{rect}(x) = \begin{cases} 1 & \text{if } |x| \leq 1, \\ 0 & \text{if } |x| \geq 1. \end{cases} \quad (5)$$

This function only acts within the Field of View (FOV) of the detector, since rays that are outside the FOV can not be received. After this has been calculated, higher order contributions can be calculated.

### II.2.2 First Order Impulse Response

In order to model the first order impulse response, the wall must be divided in facets and the contribution of each facet must be considered. The following diagram illustrates the channel:

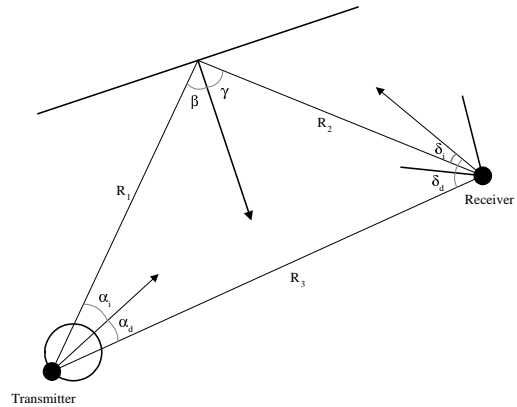


Fig. 1. Channel Diagram

In previous work [1] [9] [11] and according to Fig. 1, it has been shown that the first order impulse response is:

$$P_R = \frac{n+1}{2\pi} P_S \int_{\text{facets}} \rho \cos^n \alpha_i \cos \beta \cos \gamma \cdot \cos \delta_i \cdot \text{rect}(\delta_i) \cdot \frac{A_R}{R_1^2 R_2^2} dA \quad (6)$$

This integral sums for the contribution of all facets along the wall of interest. The significance of each facet is different, but the same calculation time is spent on any one of them.

### II.2.3 Higher Order Reflections

As mentioned in the literature, in order to calculate the  $k^{\text{th}}$  reflection, one must know the  $(k-1)^{\text{th}}$  reflection first. From [1] the following formula is used:

$$h^{(k)}(t) = \int h^{(0)}(t, Tx \rightarrow \text{facet}) \otimes h^{(k-1)}(t, \text{facet} \rightarrow Rx) dA \quad (7)$$

where  $\otimes$  denotes convolution and  $dA$  represents the facets.

This algorithm uses the line-of-sight (LOS) impulse response from the transmitter to the facet and the  $(k-1)$  impulse response from the facet to the receiver. In other words, to calculate any impulse response, one has to calculate the differential powers and delays between all the facets. This is actually the algorithm for simulating the channel [1], and for a high number of reflections or large number of facets it is inappropriate since it can lead to simulating durations of years.

## III. NOVEL WORK

This section deals with the new algorithms, which deal with delay and FOV modelling. The First order impulse response will be initially presented, followed by the higher order reflections.

### III.1 Geometric Definition of First Order Reflection

Having a fixed receiver and transmitter, the geometric locus of points that are a fixed distance from the receiver and transmitter is an ellipse in two dimensions and an ellipsoid in three dimensions. This distance represents the delay between the receiver and transmitter. Figure 2 illustrates this locus in two dimensions. Note that all rays are of the same length.

When a wall intersects the ellipsoid, the intersection forms a shape that defines all the points on the wall that are a fixed delay away from receiver and transmitter. Based on this argument, the analysis continues to first order reflection.

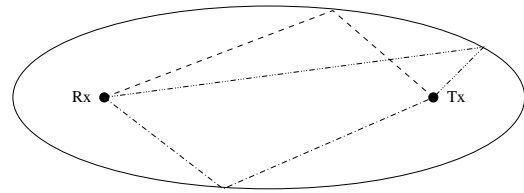


Fig. 2. Locus of points equidistant from Rx/Tx

### III.2 First order reflection

The following figure illustrates the first order reflection from a finite wall:

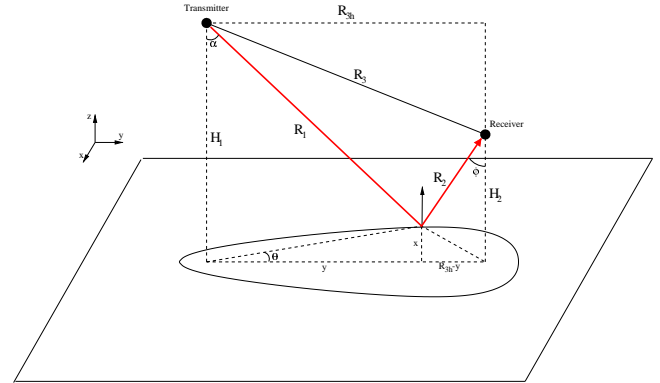


Fig. 3. Reflection from a finite wall

The shape that is drawn on the wall is again the locus of reflection points for a given delay. From this figure, we can deduce that:

$$\tau = \frac{R_1 + R_2}{c} \quad (8)$$

where  $c$  is the speed of light (m/sec) and  $\tau$  is the delay of interest (sec). Based on this argument, equation (6) can be changed so that the integrated variable is not the facet.

The goal of the novel approach is for the integration variable to be  $\theta$ . The integral will calculate the total contribution to each value of  $\tau$  in turn. time, for  $\theta = 0 \rightarrow 2\pi$ .

After some considerable manipulation (see Appendix 1), eq.6 becomes:

$$P_\tau = \frac{n+1}{2\pi^2} P_T \int_0^{2\pi} \rho \cos^{n+3}(\alpha) \cdot \frac{H_2^2 A_R dA}{H_1^2 (\tau c - \frac{H_1}{\cos \alpha})^4} \text{rect}(\delta_i) d\theta \quad (9)$$

The only unknown variable in this equation is  $\alpha$ , and this can be also found in terms of  $\theta$  by geometric manipulation. The advantage of this technique is that given a certain delay  $\tau$ , the contribution to the impulse response can be found very quickly. If, for example, the room simulated only includes time delays

ranging from 10nsec to 50nsec, it is possible to simulate only between these limits, and not for the whole room as with the facet models.

There are several ways of numerical integration that can be used to solve eq. 9, but an efficient one has been selected. It is a form of quadrature integration, and is specifically useful for trigonometric cases. Instead of integrating with 30 iterations and Simpson's rule, this technique can produce good results with 3 iterations.

### III.3 Field-of-View Modelling

In order to make analysis and simulation even more efficient and fast, it is possible to model the FOV of the receiver and transmitter. Under the assumption that the receiver and transmitter are circular elements, and their FOVs are conical (they could be pyramidal, but this would be even easier to model), the projection on the wall will always be a conic section that can be modelled. Only the reflection points that are within these areas will be considered.

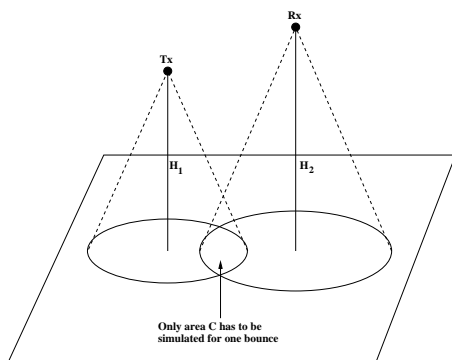


Fig. 4. Field of View Model

In the example shown above, the conic sections are circles and their equations are:

$$x_1^2 + y_1^2 = H_1^2 \quad (10)$$

$$x_2^2 + y_2^2 = H_2^2 \quad (11)$$

assuming that the coordinate system for each circle is directly below the receiver or transmitter. Since  $H_1$  and  $H_2$  are defined, the circles are also well-defined.

The point  $(x, y)$  can be easily calculated from geometry, and one can find whether any point on the wall lies inside both circles. Similarly, all conic sections can be modelled taking into account all possible receiver/transmitter orientations and positions. One must take care in the case of a hyperbola, which is symmetrical about an axis and can lead to errors. The FOV modelling technique has been included in the simulator.

### III.4 Higher Order Reflections

In order to model higher order-reflections, a solution that included both parts of the facet and delay model were considered. In order to model these reflections, one must take into account the interaction of power between the walls of the room. In order to achieve this, one must discretise the walls themselves in some way, either in facets, or in points along an ellipse. In our case, the second method was chosen.

#### III.4.1 Second order reflection

The first stage of the algorithm is similar to the first order reflection, as described above. For a given delay, a certain ellipsoid is chosen, and the intersections of this ellipsoid with the walls are found. Figure 5 illustrates this.

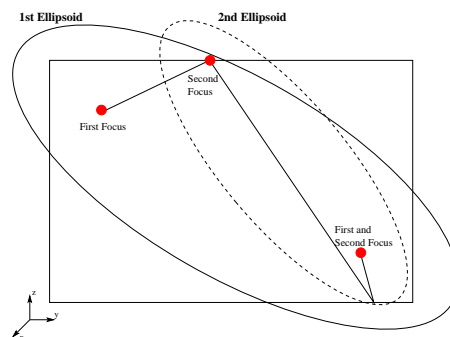


Fig. 5. Second Order Reflection

After the first ellipsoid is chosen, another ellipsoid is formed, with foci at the first point of reflection and the receiver. The first order impulse response is calculated for this ellipsoid, using the method described above. After all the points on the first intersection are calculated, the first ellipsoid is grown to include larger delays, and the second ellipsoid procedure is performed again.

This procedure may seem computationally intensive, but is still powerful, since the algorithm calculates the minimum and maximum second-reflection delays that are present in the room and only models inside these limits.

#### III.4.1 Third and higher order reflection

The method for third-order reflections is similar to the second-order, as mentioned above. The technique involving two ellipsoids is extended to include three, again calculating the minimum and maximum delays of the room beforehand. The simulation time is higher than the first and second order reflections, but is still very powerful, since only wanted calculations take place.

The algorithm can be extended to include higher order reflections, but simulation time increases along

with the number of reflections. Hence, for the purpose of this paper, the number of reflections is three.

#### IV. RESULTS

This section presents results for all the novel techniques presented above. The following table summarises the configuration of the simulations.

TABLE I  
SIMULATION PARAMETERS

Parameter	Config A LOS	Config B NLOS	Config C Phong
Room			
Length $[x, y, z]$	[5,5,5]	[4,4,4]	[4,4,4]
$\rho_{walls}$	0.8	0.3	0.12
$\rho_{ceil}$	0.8	0.56	0.3
$\rho_{floor}$	0.3	0.3	0.3
Transmitter			
Mode	1	1	1
Coordinates	[2,1,3]	[2,1,3]	[2,1,3]
Orientation	[0,0,-1]	[0,0,-1]	[0,0.33,1]
Receiver			
Area	$1cm^2$	$1cm^2$	$1cm^2$
FOV	$\pi/2$	$\pi/2$	$\pi/4$
Coordinates	[2,3,1]	[2,3,3]	[2,3,3]
Orientation	[0,0,1]	[0,0,-1]	[0,0.33,-1]

The results are presented as impulse responses, which assume that the stimulus of the channel is a unit-area Dirac function [3]. These three configurations and their impulse responses will in turn be analysed in the following sections.

##### IV.1 Configuration A

In this case, the transmitter is placed near the ceiling, while the receiver is placed near the floor of the room. They are facing each other, so that there is a LOS between them. Figure 6 illustrates the impulse response of the channel. As seen above, there is a significant amount of power in the second and third order reflections that can even be more important than the LOS component, since they produce Inter-Symbol-Interference (ISI).

The impulse response shown above is similar to the ones simulated using the conventional facet models [3], [11], but only takes a fraction of the time to simulate.

##### IV.2 Configuration B

In this case, there is no line-of-sight between the receiver and transmitter. The link relies only in higher order reflections, which is useful, since it allows the receiver or the transmitter to move freely inside the room. In our case, by placing the transmitting/receiving elements at a large distance from the

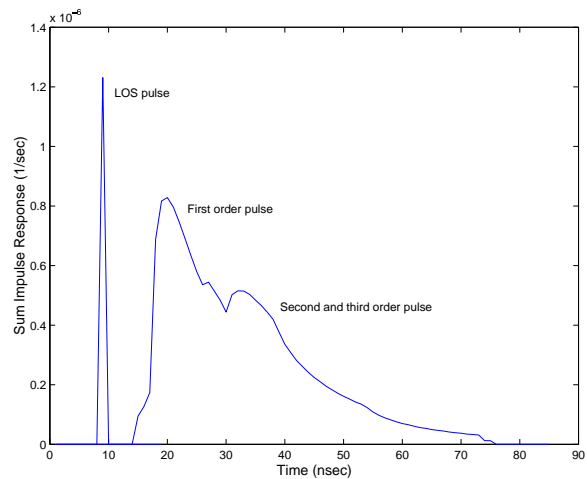


Fig. 6. Impulse Response for Configuration A

primary reflector, and facing them towards it, this reflector becomes a secondary transmitter, flooding the room with radiation if Lambert's law is chosen for the reflection model. The impulse response for this configuration is shown in Figure 7. As seen from the

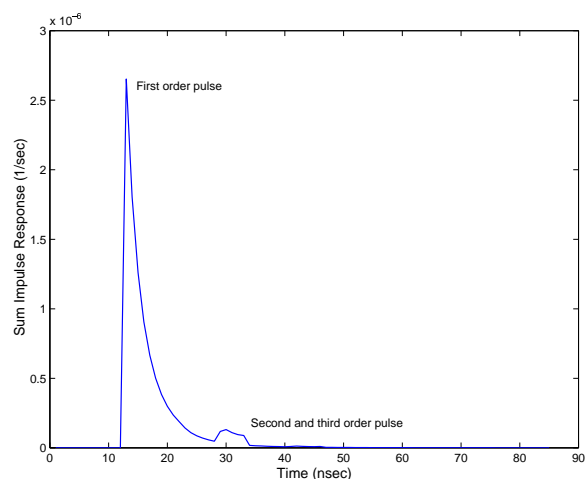


Fig. 7. Impulse Response for Configuration B

figure, the second and higher order components are weaker and do not contribute to the impulse response as before. Since the receiver has a restricted FOV ( $\pi/2$ ), it only receives high power from reflections on the primary wall, which in this case is the floor. The rest of the walls add a small response to the overall, since each ray has to travel a larger distance and is heavily attenuated by Lambert's reflection law at the points of reflection.

##### IV.3 Configuration C

This case is probably the most interesting for the purpose of this paper. It illustrates the difference if different reflection models are chosen. In previous

configuration, only Lambert's law was chosen for reflection modelling.

In this configuration, Phong's law is used. We assume that the primary reflecting wall is a perfect specular reflector, which could be a mirror or a window. Hence, it only reflects in the specular direction as described by Eq.2. The mode number for the specular component is 50, which is highly directional. In other words, only a spot on the primary reflector contributes to the impulse response and depends on this spot to maintain a link. If this spot is shadowed, the link is lost.

The receiver and transmitter are turned towards the primary reflector, and specifically towards the specular point of reflection, so that the contribution of the specular reflection is maximum. Their position is the same as the previous configuration, in order to illustrate the difference between the choice of the reflection model. Figure 8 illustrates the impulse response of this particular configuration.

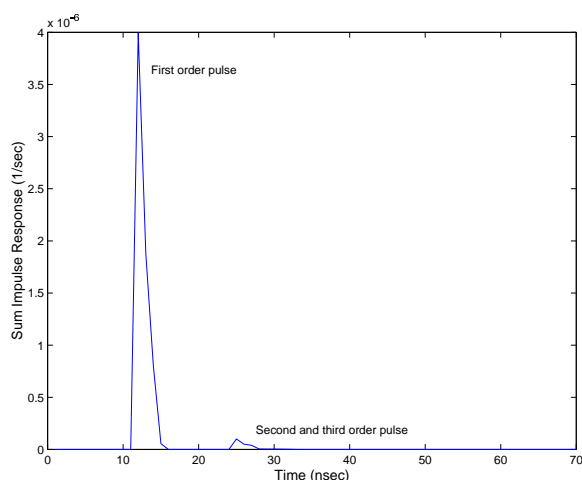


Fig. 8. Impulse Response for Configuration C

As seen from Figure 8, a significant amount of power is received, approximately an order larger than in the previous configurations. On the other hand, as mentioned above, the link depends on the specular LOS and is prone to shadowing.

When compared with the results of Configuration B, one can clearly see that more power is received and that the r.m.s. delay spread of the channel is less. Hence it is significant to include specular reflectors in the simulations and not assume that all materials conform with Lambert's law.

## V. CONCLUSION

A novel approach has been presented for calculating the impulse response of a typical infrared wireless channel. The approach is not based on discretising the simulated room into facets, but discretising the delays that are present in the channel. In this way the range of delays can be calculated in advance, and

calculations can be limited to this range. Also, one can choose which part of the impulse response, or even which reflection to calculate, making the simulation even faster and more efficient.

The results are in the form of impulse responses, under the assumption that a unit-area Dirac pulse is transmitted to the channel. The results are consistent with previous models, but only use a fraction of the processing power and duration to simulate. For the purpose of this paper, the model includes up to third order reflections, but can be modified to include higher order reflections.

Finally, the inclusion of Phong's model in the simulations proves that it may be important to model specular reflectors in the channel, and not assume that they behave as described by Lambert's law. The exclusion of such a model would result in completely false results if scatterers do indeed follow Phong's model.

## REFERENCES

- [1] J. R. Barry, J. M. Kahn, W. J. Krause, E. A. Lee, and D. G. Messerschmidt, "Simulation of multipath impulse response for indoor wireless optical channels," *IEEE Journal on Selected Areas in Communications*, vol. 11, pp. 367-379, April 1995.
- [2] B. Johnson, "Radiosity: Overview." <http://online.caup.washington.edu/courses/asch411>.
- [3] J. R. Barry, *Wireless Infrared Communications*. Kluwer Academic Publishers, 1994.
- [4] A. Suarez, E. Macias, F. J. López-Hernández, and R. Pérez-Jiménez, "Fast parallel simulation of the impulse response for infrared wireless indoor channels."
- [5] J. T. Patel, M. Govindarajan, and R. K. Shevgaonkar, "Wireless Diffuse Infrared Multipath Data Links: Channel Capacity, Eye-Safety and Receiver Design," in *AP2000 Conference*, April 2000.
- [6] F. J. López-Hernández, R. Pérez-Jiménez, and A. Santamaria, "Novel ray-tracing approach for fast calculation of the impulse response in diffuse IR-wireless indoor channels," *Proceedings of SPIE - Optical Wireless Communications II*, vol. 3850, pp. 100-107, September 1999.
- [7] M. R. Pakravan, "Estimation of indoor infrared channel parameters using neural networks," in *IEEE International Symposium on Personal, Indoor and Mobile Communications*, vol. 6, pp. 311-315, 1998.
- [8] R. Pérez Jiménez, J. Berges, and M. J. Betancor, "Statistical model for the impulse response on infrared indoor diffuse channels," *IEE Electronics Letters*, vol. 33, no. 15, pp. 1298-1301, 1997.
- [9] F. R. Gfeller and U. Bapst, "Wireless in-house data communication via diffuse infrared radiation," *Proceedings of the IEEE*, vol. 67, pp. 1474-1486, November 1979.
- [10] C. R. Lomba, R. T. Valadas, and A. M. deOliveiraDuarte, "Experimental characterisation and modelling of the reflection of infrared signals on indoor surfaces," *IEE Proceedings: Optoelectronics*, vol. 145, no. 3, pp. 191-197, 1998.
- [11] J. B. Carruthers and J. M. Kahn, "Modelling of Nondirected Wireless Infrared Channels," *IEEE Transactions on Communications*, vol. 45, pp. 1260-1267, October 1997.